Stretching-Induced Director Rotation in Thin Films of Liquid Crystal Elastomers with Homeotropic Alignment

Kenji Urayama,*,† Ryo Mashita,† Ichiro Kobayashi,‡ and Toshikazu Takigawa†

Department of Materials Chemistry, Kyoto University, Nishikyo-ku, Kyoto 615-8510, Japan, and Electronic Materials Research Laboratories, Nissan Chemical Industries, Funabashi, Chiba 273-0000, Japan

Received May 16, 2007; Revised Manuscript Received July 30, 2007

ABSTRACT: We investigate the mesogen reorientation behavior of thin films of liquid crystal elastomers (LCEs) under uniaxial elongation (*z*-axis) normal to their initial homeotropic alignment (*x*-axis). The stress−strain relation is characterized by three regions: (I) a small-strain regime exhibiting a linear relationship, (II) a moderate-strain region with a quasi-plateau stress, and (III) a large-strain region where the stress again increases. The Poisson's ratio μ_{yz} is strain-dependent: $\mu_{yz} \approx 0.17$ in region II, whereas in regions I and III, $\mu_{yz} \approx 0.5$ in accordance with that of incompressible isotropic elastomers. The considerably small μ_{yz} in region II is a consequence of the suppression of the transverse shrinkage in the *y*-direction (corresponding to the director rotation axis) during elongation. Such a deformation mode is considerably closer to pure shear than uniaxial stretching. The infrared dichroism measurement reveals that the mesogen primarily rotates within the *x*−*z* plane toward the *z*-direction in region II, whereas no further mesogen realignment takes place in region III. These results indicate that the director−rotation process is featured by a quasi-plateau stress and a pure shearlike deformation. The orientation order of the mesogens in the fully reoriented state is comparable to that in the unloaded state. The complete unloading, even after stretching up to region III, recovers the original homeotropic alignment.

Introduction

Liquid crystal elastomers (LCEs) exhibit unique stimuli-response behaviors because of their hybrid characters−a cross between liquid crystals and elastomeric solids.[1,2] A marked feature of LCEs is the strong coupling between their macroscopic shape and the orientation order of the constituent mesogenic moieties. Temperature change, electric field, and light irradiation−each of which causes the mesogen reorientation−can induce the macroscopic deformation of LCEs.[1,2] Conversely, the externally imposed deformation can drive the mesogen realignment along the stretching axis. Owing to rubber elasticity, such director switching is possible by a small load, and the original orientation can be recovered by unloading. Many researchers demonstrated a 90° rotation of the director in LCEs by stretching them normal to the initial director.[3−10] These earlier studies employed thin LCE films with a homogeneous alignment. They also noticed that the boundary conditions at the clamps significantly affect the mesogen reorientation behavior, especially when the sample strips are not sufficiently long, because the clamping at both ends of the specimens prohibits the global shear deformation induced in the course of the director rotation. The resultant mesogen reorientation becomes nonuniform and is sometimes recognized by the "stripe domain" textures. The formation mechanism of such nonuniform orientation patterns was theoretically investigated.[11−14]

The stretching of the thin LCE films with a homeotropic (normal to the film surface) alignment provides some new aspects of the director-switching behavior. This geometry can minimize the influence of such boundary conditions leading to the nonuniform mesogen reorientation because the contribution of the shear displacement ($u = \gamma \times h$ where γ is the shear strain and h is the film thickness) to the overall deformation, i.e., u/l (where l is the film length), becomes negligible for sufficiently thin films ($h/l \ll 1$). More importantly, we can readily observe the transverse dimensional change along the rotation axis of director during elongation, unlike the case of thin LCE films with a homogeneous alignment. This information is of great importance to reveal the deformation mode specific to the director rotation. There exist few experiments on the transverse dimensional changes during the stretching-induced director rotation.[5] Roberts et al.[5] observed an unusually large dimensional reduction along the initial director axis (i.e., the direction normal to the stretching axis) for a thin LCE film with a homogeneous alignment, which would be a sign of a characteristic deformation mode other than simple stretching. Unfortunately, the interpretation of their data is not straightforward because their sample of 10 mm in length and 5 mm in width was not sufficiently long enough to eliminate the boundary condition effect on the mesogen reorientation.

In the present paper, we study the stretching-induced director rotation in thin LCE films of homeotropic alignment with $h/l < 10^{-2}$. We investigate the macroscopic mechanical properties such as tensile stress and transverse dimensional changes in the director-switching process. The process of mesogen reorientation is revealed by Fourier transform infrared (FTIR) spectroscopy. We clarify the correlation of the macroscopic mechanical properties with the microscopic mesogen reorientation during elongation. We also compare the deformation mode during the director rotation induced by mechanical stretching with that observed under electric field.[15,16]

Experimental Section

Sample Preparation. The thin films of a side chain-type LCE were prepared by the photopolymerization of the reactive mesogenic monomer (Figure 1) with the cross-linker 1,6-hexanediol diacrylate (Aldrich). The reactive mesogenic monomer was synthesized using established techniques.[17] The cross-linker concentration was 10 mol % in the feed. A miscible nonreactive nematogen 4-*n*-hexyloxy-

* Corresponding author. e-mail: urayama@rheogate.polym.kyoto-u.ac.jp.
† Department of Materials Chemistry, Kyoto University.
‡ Electronic Materials Research Laboratories, Nissan Chemical Industries.

10.1021/ma071104y CCC: $37.00
Published on Web 09/12/2007

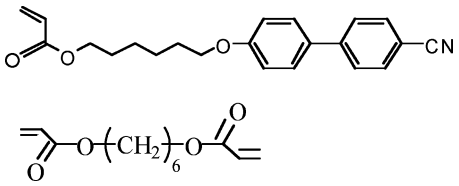

Figure 1. Chemical structures of employed mesogenic monomer and cross-linker.

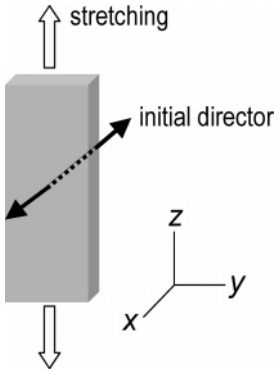

Figure 2. Stretching of LCE films with a homeotropic alignment.

4′-cyanobiphenyl was mixed with the reactive monomer by a molar ratio of 50:50 to broaden the temperature range of the nematic phase. The reactant mixture was sandwiched between two glass plates separated by 60 μm-thick spacers. The plates were coated with a polyimide layer (provided by Nissan Chemical) that induces the normal (homeotropic) alignment of the nematogens to the layer surface. The photopolymerization was carried out at 45 °C in the nematic state of the mixture using Irgacure 784 as a photoinitiator. The cell was irradiated using a xenon lamp with emissions at a wavelength of 526 nm for 15 min. The resulting gel films were detached from the glass substrates by immersing the sandwiched cell in dichloromethane for half a day. The unreacted and nonreactive materials were washed out by the swelling of the detached films in dichromethane. The swollen gel film was gradually deswollen by increasing the methanol content in the swelling solvent. The LCE film was obtained by drying the deswollen gel in air. The rectangular sample strips of about 15 mm in length and 2 mm in width with a thickness of 45 μm for the tensile and IR dichroism measurements were cut from the same large dry film. The nematic−isotropic transition (T_{NI}) and glass transition temperatures of the LCE film were 95 °C and approximately 50 °C, respectively.

Tensile Measurements. The tensile measurements of the film specimens were conducted with a UTM-500 equipped with a temperature-controllable box. The both edge areas (about 2 × 2 mm) of the specimens were mechanically clamped, so that the effective initial length in the stretching direction was about 10 mm. The considerably large ratio of the effective length to the width (ca. 5) is expected to provide sufficient freedom to lateral displacement by stretching except for the vicinity of the clamped region. The specimen was uniaxially stretched in the *z*-direction normal to the initial director in the *x*-direction (Figure 2). The slowest available cross-head speed of the tensile tester (0.5 mm/min) was employed to adjust to the considerably slow strain rate in the IR dichroism measurement (as described later). The stretching process was recorded by a video camera. The dimensional variations in the *y*- and *z*-directions during elongation were evaluated by video analysis.

Infrared Dichroism Measurements. The IR dichroism measurement of the LCE films under tension was conducted using a custom-built stretching device. The film specimen was clamped at both ends in the same manner as in the tensile measurement. These clamps were shiftable by micrometer screws, so that the imposed strain could be controlled with high precision and the beam spot (1 mm in diameter) on the central part of the specimen could remain at the same position during elongation. The beam spot on the specimen was considerably distant from the clamped regions to minimize the effect of the boundary condition on the mesogen reorientation in the area of interest. The stretching setup equipped with a temperature-controllable box was integrated into an FTIR spectrometer Jasco 4200ST. The adsorption band of the terminal CN group parallel to the long axis of the mesogen was used to characterize the orientation order of the mesogen. The absorbances of the incident polarized light parallel and normal to the stretching direction (denoted by A_z and A_y, respectively) were measured as a function of the tensile strain. The stretching was conducted stepwise with each step consisting of approximately a 5% strain increase, because the measurement required approximately 5 min at each strain to acquire the data with a sufficiently high signal-to-noise ratio. The average stretching rate of the entire process (approximately 2×10^{-4} s^{-1}), including the measurement times, was of the same order as that in the tensile measurements (8×10^{-4} s^{-1}).

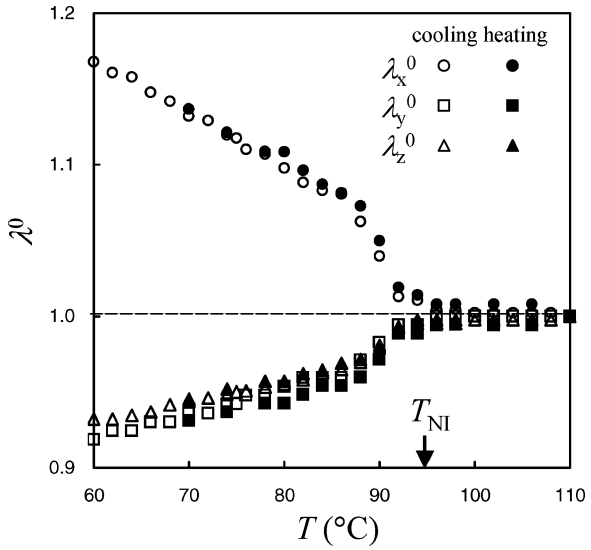

Figure 3. Temperature dependence of principal ratios λ_i^0 ($i = x, y, z$) in the unloaded state. The reference state of λ_i^0 is the isotropic state at 110 °C.

Results and Discussion

Thermally Induced Shape Variation in the Unloaded State. Figure 3 shows the equilibrium principal ratios λ_i^0 ($i = x, y, z$) of the thin LCE film without an external load as a function of temperature (T). The dimensions at 110 °C in the isotropic state are chosen as the reference state for λ_i^0. The ratio λ_x^0 in the thickness direction was calculated by $\lambda_x^0 = (\lambda_y^0 \lambda_z^0)^{-1}$ on the basis of the volume constancy. The volume conservation is reasonably assumed because the system is in the rubbery state at the temperatures of interest. In the nematic state of $T < T_{NI}$, the specimen uniaxially elongates in the thickness direction ($\lambda_x^0 > 1$ and $\lambda_y^0 \approx \lambda_z^0$), and the elongation increases with a decrease in T. The distortion is thermally reversible for the temperature changes across T_{NI}. A similar thermal deformation was reported previously for various LCEs with homogeneous alignment.[1,18] The results in Figure 3 confirm the presence of a global director in the thickness direction (i.e., homeotropic mesogen alignment) in the unloaded state.

Figure 4 displays the T dependence of the order parameter S_x^0 of the mesogen in the thickness direction that was estimated from the absorbance A_y^0 for the specimen without an external load. The order parameter is defined by $S_x^0 = 3\langle\cos^2\theta\rangle/2 - 1/2$ where θ is the angle between the long axis of the mesogen and the *x*-axis and $\langle\cos^2\theta\rangle$ is the mean value of $\cos^2\theta$. The absorbances A_y^0 and A_z^0 at each T were almost identical. This

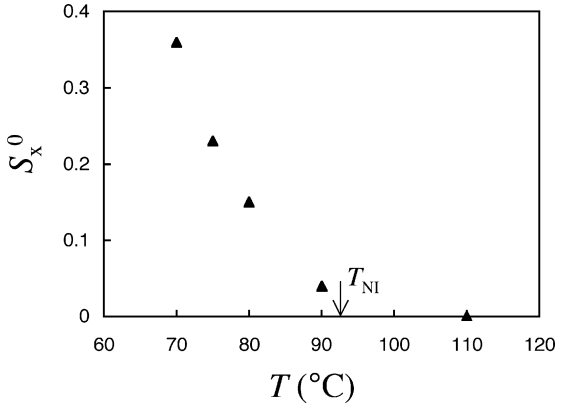

Figure 4. Temperature dependence of the order parameter of the mesogens S_x^0 in the unloaded state evaluated from the absorbance data.

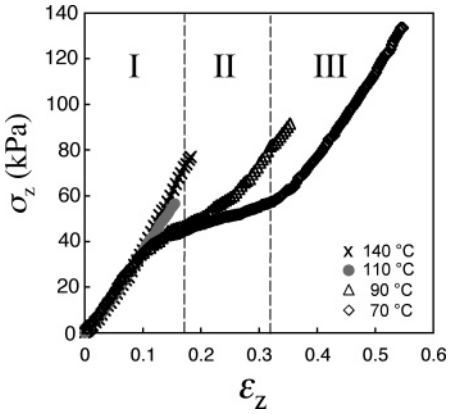

Figure 5. Stress−strain curves at various temperatures, where the stress is the nominal stress and the strain is the true strain. Regions I, II, and III are based on the ϵ_z dependence of ϵ_y at 70 °C in Figure 6.

indicates the uniaxial orientation of the mesogens along the *x*-axis. In such systems, A_y^0 is correlated with the orientation distribution function of the transition moment $f(\theta)$ as $A_y^0 = (M/2)^2 \int f(\theta) \sin^2 \theta \, d\theta$ where M is the absolute magnitude of transition moment.[19] The values of $S_x^0(T)$ were calculated from $A_y^0(T)$ and A_y^0 in the high-temperature isotropic state (110 °C) with random orientation ($\langle \cos^2 \theta \rangle = 1/3$). In the calculation, $A_y^0(T)$ was reduced by $\lambda_x^0(T)$ (Figure 3) to consider the variations in the effective optical path caused by thermal deformation. As observed in Figure 4, S_x^0 increases with cooling. An increase in S_x^0 upon cooling leads to the spontaneous stretching in the thickness direction (Figure 3).

Stress—Strain Behaviors. Figure 5 displays the stress−strain curves at various temperatures. The stress is the nominal stress, and the strain (ϵ) is the true strain given by $\epsilon = \ln \lambda$, where λ is the principal ratio. The ratio λ is defined by $\lambda = l/l_0$ where l and l_0 are the dimensions in the stretched and relaxed states, respectively. The stress−strain relation in the isotropic state at $T > T_{NI}$ has no singularity. It is almost linear over the entire strain region, although the specimens are not highly extensible. The shape of the stress−strain curves in the nematic state significantly differs from that in the isotropic state. The stress−strain curves in the nematic state are characterized by three regions: (I) the small-strain region exhibiting linear elasticity, (II) the moderate-strain region with a quasi-plateau stress, and (III) the large-strain region where the stress again increases. The stress−strain curves at different values of T in the nematic state are similar in their shapes as well as quasi-plateau stresses, but the quasi-plateau region becomes broader with a decrease in T, i.e., an increase in S_x^0. The strain-rate effect on the stress−strain behavior was not explored in detail in the present study; however, no significant difference was observed in the stress−strain curves at 70 °C for the strain rates of 8×10^{-4} s^{-1} and 8×10^{-3} s^{-1}. The initial Young's modulus given by the slope at the small strains is approximately 300 kPa and it does not significantly depend on T in the T range examined here.

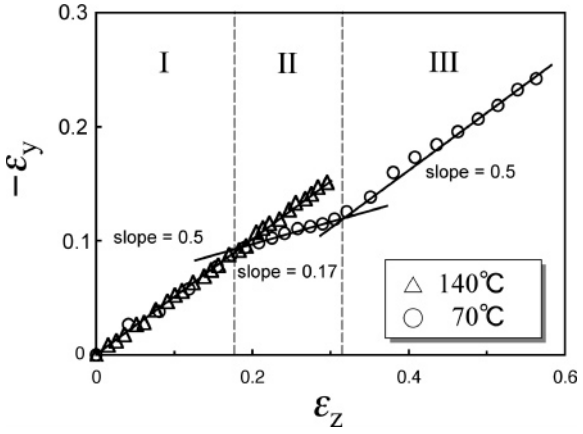

Figure 6. Relation of the true strains in the *y*- and *z*-directions during stretching. The slope corresponds to the Poisson's ratio μ_{yz}.

Poisson's Ratio μ_{yz}. Figure 6 shows the relations between the true strains in the *y*- and *z*-directions at 70 °C and 110 °C. The slope of this plot corresponds to the Poisson's ratio μ_{yz} ($\mu_{yz} = -d\epsilon_y/d\epsilon_z$). In the isotropic state (110 °C), all data points fall on the straight line with a slope of 0.5, i.e., $\mu_{yz} = 0.5$. This behavior is identical with that of incompressible isotropic elastomers,[20] and the dimensions in the two transverse directions during stretching decrease equivalently. In contrast, μ_{yz} in the nematic state is strain-dependent. In the small- and large-strain regions of $\epsilon_z < 0.18$ and $\epsilon_z > 0.32$, respectively, μ_{yz} is well approximated to be 0.5, but μ_{yz} ($\approx$0.17) at the intermediate-strain region ($0.18 < \epsilon_z < 0.32$) exhibiting the quasi-plateau stress (Figure 5) becomes considerably smaller than 0.5. This small μ_{yz} indicates that the dimensional reduction in the *y*-direction caused by stretching is significantly suppressed. The dimensional reduction in the thickness (x) direction at the corresponding strains becomes larger owing to volume conservation: μ_{xz} is evaluated to be 0.83 from $\lambda_x\lambda_y\lambda_z = \lambda_z^{(1-\mu_{xz}-\mu_{yz})} = 1$. This deformation mode is considerably closer to pure shear ($\mu_{yz} = 0$ and $\mu_{xz} = 1$) rather than simple uniaxial stretching ($\mu_{xz} = \mu_{yz} = 0.5$) for incompressible materials. The pure shear deformation of isotropic elastomers is usually achieved by "constrained" uniaxial stretching, where a mechanical constraint is imposed on the specimens such that no dimensional change in one of the two transverse directions can occur.[20,21] It should be noted that this pure shearlike deformation in the nematic elastomers arises even though the externally imposed deformation is simple uniaxial stretching with no constraint on lateral shrinkage.

Infrared Dichroism. Figure 7a illustrates the ϵ_z dependence of the dichroic ratio $D_{z,y} = A_z/A_y$ at 70, 90, and 110 °C. In the undeformed state, $D_{z,y} \approx 1$; the mesogen alignment in the $y-z$ plane before stretching is random even in the nematic state owing to uniaxial orientation about the *x*-axis. In the isotropic state (110 °C), $D_{z,y}$ remains almost unity even at large elongation. The stretching in the isotropic state induces no appreciable orientation of the dangling mesogens.

In the nematic state (70 and 90 °C), $D_{z,y}$ increases with stretching, and becomes constant in the sufficiently high strain region. The corresponding order parameter $S_z = (D_{z,y} - 1)/(D_{z,y} + 2)$ along the stretching axis in the plateau region is 0.36

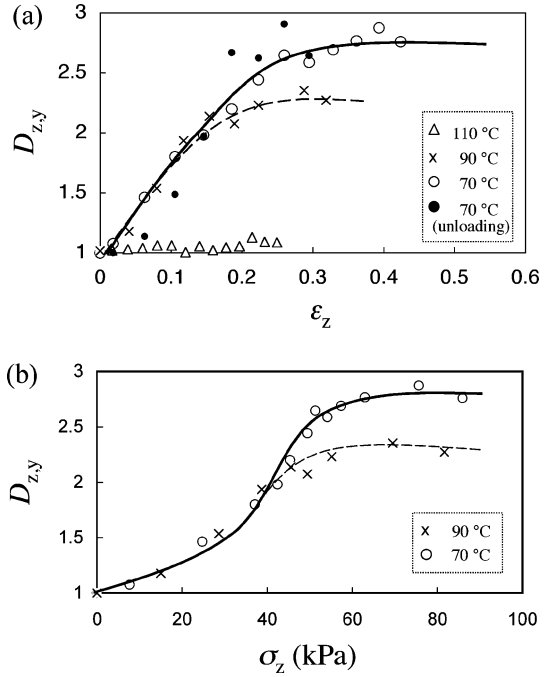

Figure 7. Dichroic ratio $D_{z,y}$ at various temperatures as a function of (a) the strain ϵ_z and (b) the stress σ_z.

and 0.29 at 70 and 90 °C, respectively, each of which is similar to (70 °C) or considerably higher than (90 °C) that in the unloaded state (S_x^0). This result clearly indicates that the elongation drives the realignment of the dangling mesogens along the stretching direction. At the large strains where the stress increases again (Figure 5) with $\mu_{yz} = 0.5$ (Figure 6), no further mesogen realignment occurs. The saturation of $D_{z,y}$ at 90 °C takes place at the smaller strain ($\epsilon_z \approx 0.22$) than that at 70 °C ($\epsilon_z \approx 0.32$). This agrees with the result that the stress upturn at 90 °C begins at the smaller strain ($\epsilon_z \approx 0.20$) than that at 70 °C ($\epsilon_z \approx 0.35$).

The data in the unloading process from $\epsilon_z = 0.42$ at 70 °C are also shown in Figure 7a. The mesogen orientation recovers the initial state ($D_{z,y} = 1$) when the imposed strain is completely removed, although a finite difference in the ϵ_z dependence of $D_{z,y}$ is observed in the loading and unloading processes. This result demonstrates that the director is mechanically switchable by the imposition and removal of the tensile strain.

Figure 7b shows $D_{z,y}$ as a function of σ_z at 70 °C and 90 °C. In the high stress region, the stress increase causes no further increase in $D_{z,y}$. This feature is essentially the same as that in Figure 7a using strain as a variable. Importantly, a rapid increase in $D_{z,y}$ is observed around 40 kPa, i.e., corresponding to the quasi-plateau stress in Figure 5. This shows that a significant degree of mesogen realignment occurs under the quasi-plateau stress.

Correlation between Mechanical Properties and Mesogen Reorientation. The ϵ_z dependencies of A_y and A_z are more informative than that of the ratio $D_{z,y}$ for the detailed exploration of the reorientation behavior. Figure 8 displays A_y and A_z as a function of ϵ_z at 70 °C. The data at each strain are reduced by λ_x to consider a reduction in the effective optical path by elongation, and λ_x was calculated from the data in Figure 6 assuming volume constancy. The strain region I ($\epsilon_z < 0.18$), region II ($0.18 < \epsilon_z < 0.32$), and region III ($\epsilon_z > 0.32$), according to the ϵ_z dependence of μ_{yz} (Figure 6), are indicated in Figures 5 and 8 to discuss the correlation between the mechanical properties (σ_z and μ_{yz}) and reorientation behaviors (A_y and A_z). As observed in Figure 8, each regime exhibits the

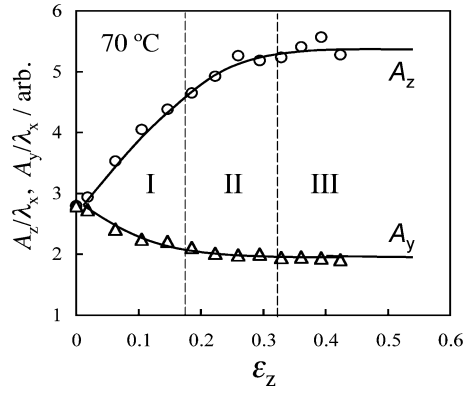

Figure 8. Strain dependence of the absorbances A_y and A_z at 70 °C, where A_y and A_z are reduced by λ_x to consider the variation in the effective optical path during elongation. Regions I, II, and III are based on the ϵ_z dependence of ϵ_y in Figure 6.

characteristic ϵ_z dependencies of A_y and A_z. With increasing ϵ_z, (i) A_y decreases and A_z increases in region I, (ii) A_z increases with no change of A_y in region II, and (iii) neither A_y nor A_z changes in region III. In particular, such ϵ_z dependencies of A_y and A_z in region II indicate the characteristic mode of the mesogen reorientation, i.e., the mesogen primarily rotates in the $x-z$ plane toward the stretching direction. The quasi-plateau stress at the corresponding strains indicates that this director rotation is readily induced by a constant stress (approximately 40 kPa in the present case) and that it occurs cooperatively. This director rotation in the $x-z$ plane is also responsible for the pure shearlike deformation mode (the small μ_{yz}) in region II.

The coexistence of the symmetric rotation states of $+\theta$ and $-\theta$ before stretching is expected because of $A_y^0 \approx A_z^0$ and $S_x^0 \neq 1$ in the relaxed state (Figure 4). Both states, however, lead to essentially the same deformation mode. The similar deformation mode is observed for an unconstrained LCE subjected to a 90° rotation of the director under an electric field;[15,16] the induced deformation is pure shear ($\mu_{yz} = 0$), i.e., the LCE is elongated along the field axis but with no dimensional variation in the direction regarding the director rotation axis (in other words, the direction perpendicular to the plane where the director stays confined during rotation). The present result shows that the pure shearlike deformation mode also arises when the director is rotated by mechanical uniaxial stretching. This similarity suggests that the director rotation in LCEs is always accompanied by pure shear deformation. A finite deviation ($\mu_{yz} \neq 0$) from pure shear in the mechanically driven director rotation is probably because the macroscopic dimensional change (ϵ_y) in the elastomers is directly influenced by the externally imposed uniaxial stretching. In contrast, under electric fields the pure shear mode specific to director rotation is clearly visible because the imposed fields influence the mesogen orientation but do not directly deform the elastomers. A finite effect of the boundary conditions at clamps on μ_{yz} cannot be completely ruled out here although the specimen length is considerably (ca. five times) longer than its width. The experiments for the specimens with various dimensional ratios will reveal such boundary condition effect.

In region I, A_z increases with elongation but is accompanied by a reduction in A_y. This behavior indicates that the mesogens are reoriented along the stretching axis in the $y-z$ plane. The mesogen alignment in the $y-z$ plane is varied from the random state ($D_{z,y} = 1$) to a considerably ordered state ($D_{z,y} \approx 2.2$) by the stretching of $\epsilon_z = 0.18$ (the end of region I). This implies that a finite mesogen orientation in the $y-z$ plane is needed for

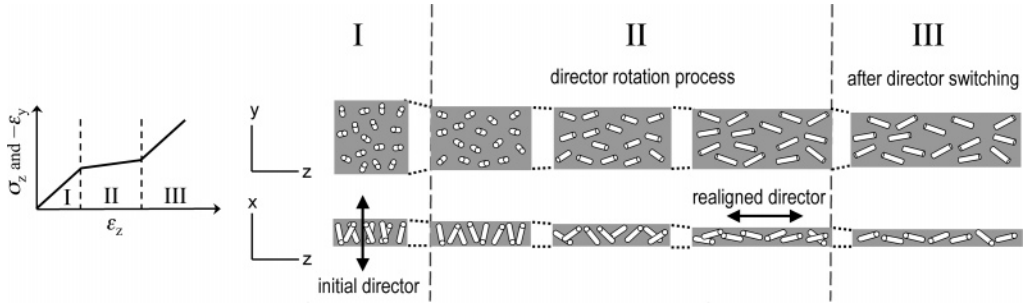

Figure 9. Schematics for the correlation of the macroscopic deformation with the microscopic mesogen reorientation.

the occurrence of the cooperative director rotation in the $x-z$ plane in region II. The variation in A_z in region I may also include a finite mesogen orientation in the $x-z$ plane, leading to an A_z increase with no A_y change. However, the mechanical behaviors with no singularity (linear stress−strain relation and $\mu_{yz} = 0.5$) suggest that the degree of the director rotation in the $x-z$ plane, if any, is considerably smaller in region I because it results in unusual mechanical behaviors as observed in region II. It should be noted that the presence of a finite ordering process in the $y-z$ plane prior to the cooperative director rotation (region I) may be due to the relatively low nematic order of the present specimen ($S_x^0 \approx 0.3$). In a highly oriented homeotropic LCE, the mesogen orientation may occur only in the x-z plane without that in the $y-z$ plane (i.e., only A_z varies with no A_y change) in the stretching process. In such cases, the induced deformation may also become closer to pure shear ($\mu_{yz} \rightarrow 0$).

In region III, the stretching does not lead to further variations in either A_y or A_z. This implies that the director rotation is completed at the end of region II, and region III corresponds to the past director-switching regime. The stress increase in region III is entirely due to the entropic elasticity of the stretched network chains. The macroscopic deformation behavior in region III becomes the classical response ($\mu_{yz} = 0.5$) once again. Figure 9 shows the schematics for the correlation between the mesogen reorientation and the macroscopic shape during stretching.

Finally, we compare the present results with the expectations of the soft elasticity theory for nematic elastomers.[1,22−24] The theory expects the presence of the "soft mode" in the process of director rotation−a route at no cost or a significantly low-energy cost for the transition between the initial and 90° rotation states of the director. The macroscopic deformation via the soft mode under imposed uniaxial tension is pure shear ($\epsilon_y = 0$ in the present notation).[24] The full soft mode scenario leads to $\sigma_z = 0$ and $\mu_{yz} = 0$ during the director rotation. A significant reduction in tensile stress is observed as a quasi-plateau stress (approximately 40 kPa) in the director rotation process. The "semi-soft" concept considers that the quasi-plateau stress (the significantly low modulus given by the slope in this region) is a sign of the softness and it attributes the finite stress to the deviation from the ideal soft response owing to structural imperfections formed by cross-linkng in the aligned nematic state.[1] We notice the similarity in the deformation mode between the experiment ($\mu_{yz} \approx 0.17$, pure shearlike deformation) and theory ($\mu_{yz} = 0$, pure shear). The theory[24] also correlates the value of the strain at which the director rotation is complete with the shape anisotropy of the constituent nematic network chains: the rotation ends at $\epsilon_z^{II} = \epsilon_z^{I} + \ln k$, where ϵ_z^{I} is the true strain at the beginning of rotation and k is a measure of shape anisotropy. The strain region corresponding to the director rotation becomes wider with an increase in nematic order. For 70 °C, with $\epsilon_z^{I} \approx 0.18$ and $k = 1.20$, the predicted end of region II would be around $\epsilon_z^{II} \approx 0.35$, similar to the data in Figures 5 and 6 ($\epsilon_z^{II} \approx 0.32$); for 90 °C, with $k = 1.07$, it should be around $\epsilon_z^{II} \approx 0.25$, close to the data in Figure 5 ($\epsilon_z^{II} \approx 0.21$). The values of k were estimated by the theoretical relation[1] of $\lambda_x^0 = k^{2/3}$ with the data in Figure 3. For the estimation of k, it is more appropriate to use λ_x^0, which is directly related to the orientation order of the network backbone, as compared to S_x^0, which represents that of dangling mesogens.

Conclusions

When a thin film of LCEs having homeotropic alignment is stretched normal to the initial director, the director is realigned along the stretching axis at a sufficiently large elongation. The orientation order in the sufficiently stretched state is comparable to that in the unloaded state. The director reorientation process is characterized by the three strain regimes. In the small-strain regime ($\epsilon_z < \epsilon_z^{I}$), the mechanical behavior is identical to that of isotropic elastomers; the stress−strain relation is linear and the Poisson's ratio μ_{yz} is 0.5. In this regime, the mesogen orientation changes primarily in the $y-z$ plane from the random state to a finitely aligned state along the stretching axis.

In the moderate-strain region ($\epsilon_z^{I} < \epsilon_z < \epsilon_z^{II}$), the stress is almost constant (ca. 40 kPa), and $\mu_{yz}(\approx 0.17)$ becomes considerably smaller than 0.5. In this region, the mesogen rotation occurs primarily in the $x-z$ plane. The small plateau stress suggests that such mesogen rotation proceeds cooperatively. We point out the similarity between this pure shearlike deformation and the pure shear mode observed in the unconstrained LCEs subjected to a 90° director rotation under an electric field. This similarity indicates that pure shear always accompanies the director rotation in LCEs. The feature of the deformation mode in the director rotation process is similar to the picture of the soft elasticity theory expecting a route at significantly low-energy cost.

In the large-strain region ($\epsilon_z > \epsilon_z^{II}$), the stress increases again but without any further mesogen realignment. The stress increase is entirely due to the entropic elasticity of stretched network chains. The homeotropic mesogen alignment before elongation is recoverable after complete unloading, even from the highly stretched state.

Acknowledgment. The authors would like to express their gratitude to Prof. K. Nitta and Dr. T. Kawamura in Kanazawa University for their helpful suggestions regarding the FTIR measurements. The authors would also like to thank Chiba Specialty Chemicals Co. for providing the photoinitiator. This work was partly supported by a Grant-in-Aid for Scientific Research (B) (No. 16750186) and one on Priority Area "Soft Matter Physics" (No. 19031014) from the Ministry of Education, Culture, Sports, Science, and Technology of Japan.

References and Notes

(1) Warner, M.; Terentjev, E. M. *Liquid Crystals Elastomers*; Clarendon Press: London, 2003.
(2) Urayama, K. *Macromolecules* **2007**, *40*, 2277.
(3) Mitchell, G. R.; Davis, F. J.; Guo, W. *Phys. Rev. Lett.* **1993**, *71*, 2947.
(4) Kundler, I.; Finkelmann, H. *Macromol. Rapid Commun.* **1995**, *16*, 679.
(5) Roberts, P. M. S.; Mitchell, G. R.; Davis, F. J. *J. Phys. II (Paris*) **1997**, *7*, 1337.
(6) Kundler, I.; Finkelmann, H. *Macromol. Chem. Phys.* **1998**, *199*, 677.
(7) Zubarev, E. R.; Talroze, R. V.; Yuranova, T. I.; Plate, N. A.; Finkelmann, H. *Macromolecules* **1998**, *31*, 3566.
(8) Clarke, S. M.; Hotta, A.; Tajbakhsh, A. R.; Terentjev, E. M. *Phys. Rev. E* **2001**, *64*, 061702.
(9) Tammer, M.; Li, J. J.; Komp, A.; Finkelmann, H.; Kremer, F. *Macromol. Chem. Phys.* **2005**, *206*, 709.
(10) Zhang, F.; Heiney, P. A.; Srinivasan, A.; Naciri, J.; Ratna, B. *Phys. Rev. E* **2006**, *73*, 021701.
(11) Bladon, P.; Terentjev, E. M.; Warner, M. *J. Phys. II (Paris*) **1994**, *4*, 75.
(12) Weilepp, J.; Brand, H. R. *Europhys. Lett.* **1996**, *34*, 495.
(13) Conti, S.; DeSimone, A.; Dolzmann, G. *J. Mech. Phys. Solids* **2002**, *50*, 1431.
(14) Conti, S.; DeSimone, A.; Dolzmann, G. *Phys. Rev. E* **2002**, *66*, 061710.
(15) Urayama, K.; Honda, S.; Takigawa, T. *Macromolecules* **2005**, *38*, 3574.
(16) Urayama, K.; Honda, S.; Takigawa, T. *Macromolecules* **2006**, *39*, 1943.
(17) Shibaev, V. P.; Kostromin, S. G.; Plate, N. A. *Eur. Polym. J.* **1982**, *18*, 651.
(18) Kupfer, J.; Finkelmann, H. *Makromol. Chem. Rapid Commun.* **1991**, *12*, 717.
(19) Siesler, H. W. *Infrared and Raman Spectroscopy of Polymers*; Marcel Dekker: New York, 1980.
(20) Treloar, L. R. G. *The Physics of Rubber Elasticity*, 3rd ed.; Clarendon Press: Oxford, U.K., 1975.
(21) Urayama, K. *J. Polym. Sci., Part B: Polym. Phys.* **2006**, *44*, 3440.
(22) Golubovic, L.; Lubensky, T. C. *Phys. Rev. Lett.* **1989**, *63*, 1082.
(23) Warner, M.; Bladon, P.; Terentjev, E. M. *J. Phys. II (Paris*) **1994**, *4*, 93.
(24) Verwey, G. C.; Warner, M.; Terentjev, E. M. *J. Phys. II (Paris*) **1996**, *6*, 1273.

MA071104Y